Mechanistic Studies on the Hexadecafluorophthalocyanine–Iron-Catalyzed Wacker-Type Oxidation of Olefins to Ketones**

Florian Puls,[a] Felix Seewald,[b] Vadim Grinenko,[b] Hans-Henning Klauß,[b] and Hans-Joachim Knölker*[a]

Dedicated to Professor Yasuyuki Kita on the occasion of his 77th birthday

Abstract: The hexadecafluorophthalocyanine–iron complex $FePcF_{16}$ was recently shown to convert olefins into ketones in the presence of stoichiometric amounts of triethylsilane in ethanol at room temperature under an oxygen atmosphere. Herein, we describe an extensive mechanistic investigation for the conversion of 2-vinylnaphthalene into 2-acetylnaphthalene as model reaction. A variety of studies including deuterium- and $^{18}O_2$-labeling experiments, ESI-MS, and ^{57}Fe Mössbauer spectroscopy were performed to identify the intermediates involved in the catalytic cycle of the oxidation process. Finally, a detailed and well-supported reaction mechanism for the $FePcF_{16}$-catalyzed Wacker-type oxidation is proposed.

Introduction

The selective oxidation of organic substrates by using earth-abundant transition metals (e.g., manganese, cobalt or iron) as catalysts and environmentally benign oxidants (molecular oxygen or hydrogen peroxide) is fundamentally important in biogenetic transformations and highly useful for organic synthesis.[1] Olefins are readily available substrates not only in research laboratories but also for industrial processes. Thus, the selective functionalization of these basic chemicals is an important conversion for preparative organic chemistry. In this context, the hydrofunctionalization of olefins by catalysis with first-row transition metals has become a powerful tool for the successful construction of C–C and C–X bonds (e.g., X = NR_2, SiR_3, F, Cl, N_3).[2] However, the conversion of olefins into ketones in a Wacker-type oxidation is mostly limited to palladium with only a few exceptions (Scheme 1).

Based on earlier work by Tabushi and Koga, Perrée-Fauvet and Gaudemer reported in 1981 a catalytic oxidation of olefins to a mixture of ketones and the corresponding alcohols using a porphyrin–manganese(III) complex.[3] In 1992, Matsushita and co-workers reported the conversion of olefins into ketones as major product along with hydroperoxides and alcohols as by-products using a porphyrin–cobalt(II) complex as catalyst in the presence of triethylsilane and molecular oxygen at room temperature.[4] Alternative procedures for the oxidation of olefins to ketones catalyzed by base metals proceed via the transformation of intermediate secondary alcohols,[5] hydroperoxides,[6] vinyl silanes,[7] or silylperoxides.[8] In further publications, the ketone was obtained only as a by-product.[9]

Aldehyde-selective Wacker-type oxidations catalyzed by cobalt or iron complexes have been described in the literature.[10] However, iron-catalyzed Wacker-type oxidations for the conversion of alkenes into ketones are rare. Recently, Han

[a] Dr. F. Puls, Prof. Dr. H.-J. Knölker
Fakultät Chemie, Technische Universität Dresden
Bergstraße 66, 01069 Dresden (Germany)
E-mail: hans-joachim.knoelker@tu-dresden.de
Homepage: http://www.chm.tu-dresden.de/oc2/

[b] F. Seewald, Dr. V. Grinenko, Prof. Dr. H.-H. Klauß
Institute of Solid State and Materials Physics
Fakultät Physik, Technische Universität Dresden
Zellescher Weg 16, 01069 Dresden (Germany)
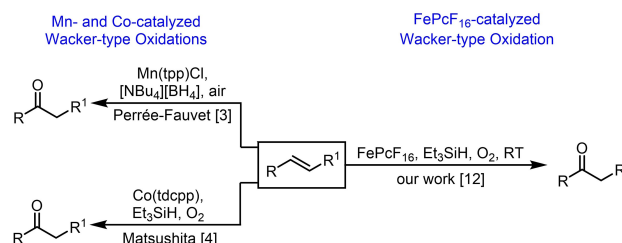
Scheme 1. First-row transition metal-catalyzed oxidations of olefins to ketones. Mn(tpp)Cl = 5,10,15,20-tetraphenylporphyrin–manganese(III) chloride; Co(tdcpp) = 5,10,15,20-tetrakis(2,6-dichlorophenyl)porphyrin–cobalt (II); $FePcF_{16}$ = hexadecafluorophthalocyanine–iron(II).

Chemistry–A European Journal

Full Paper
doi.org/10.1002/chem.202102848

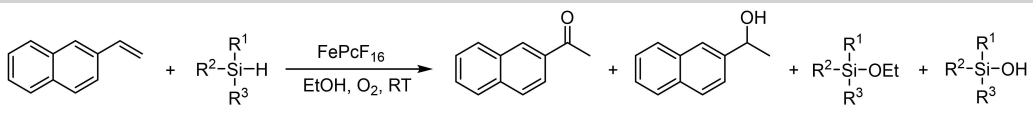**Chemistry Europe**
European Chemical
Societies Publishing

et al. and our group independently developed two procedures for the iron-catalyzed Wacker-type conversion of olefins into ketones.[11,12] Han and co-workers used 10 mol% of iron(II) chloride in the presence of polymethylhydrosiloxane (PMHS) at 80 °C.[11] We reported a procedure using hexadecafluorophthalo-cyanine–iron(II) (FePcF$_{16}$)[13] as catalyst in the presence of triethylsilane that is operating at room temperature.[12] More recently, we also described tris(1,3-diketonato)iron(III) complexes, and a combination of iron(II) chloride and neocuproine as catalysts using phenylsilane as reductive additive for the Wacker-type oxidation with air as oxidant at room temperature.[14]

Although first-row transition metal catalysis has received much attention for the hydrofunctionalization of olefins,[2f,g,15] its application for the Wacker-type oxidation to ketones is less explored. In the course of our on-going project directed towards the development of novel environmentally benign and sustainable iron-catalyzed processes,[12,14,16] we have investigated the mechanism of the FePcF$_{16}$-catalyzed Wacker-type oxidation of olefins to ketones in the presence of hydrosilanes as reducing additives at room temperature. Herein, the characterization of catalytically relevant iron complexes and intermediates, isotopic labeling studies, and Mössbauer spectroscopy of the iron complexes are described. Based on the experimental findings, a detailed mechanism has been proposed for the FePcF$_{16}$-catalyzed Wacker-type oxidation.

Results and Discussion

The iron-catalyzed Wacker-type oxidation of 2-vinylnaphthalene (**1**) using FePcF$_{16}$ as catalyst (5 mol%) in the presence of triethylsilane (**2a**) (2 equiv) in ethanol at room temperature under an atmosphere of molecular oxygen provided 2-acetylnaphthalene (**3**) in 82% yield along with 1-(2-naphthyl)-ethanol (**4**) in 12% yield (Table 1, entry 1).[12] An oligomerization of **1** was not observed under these reaction conditions. Extra dry ethanol (water content: 6.5 ppm, determined by Karl–Fischer titration) as solvent is not required as it gave the same result as ethanol of 98% purity. As 2-vinylnaphthalene (**1**) and the resulting products **3** and **4** are all solid compounds, we selected **1** as model substrate. We have investigated this reaction in detail by testing various hydrosilanes **2** as reductive additives (Table 1, entries 1–17). Except for iPr$_3$SiH (**2b**) (entry 3) and (TMS)$_3$SiH (**2c**) (entry 4),[17] the ketone **3** was isolated in moderate to good yields along with the alcohol **4** as by-product. With triethoxysilane (**2d**) as reductive additive, elevated temperatures are required to obtain at least moderate yields of the ketone **3** (compare Table 1, entries 5 and 6). Working at room temperature, the arylhydrosilanes **2e–2k** (entries 7–17) are superior additives for this reaction and in most cases the corresponding ethoxysilanes **5** and silanols **6** could be isolated. Using triphenylsilane (**2k**) as reductive additive for the oxidation of **1**, the ketone **3** was afforded in slightly better yield and in significantly shorter reaction time as compared to the reaction with triethylsilane (**2a**) (compare Table 1, entries 1 and 13, Figure 1). This beneficial effect was already noted previously in our improved synthesis of the

Table 1. Variation of hydrosilane **2** for the FePcF$_{16}$-catalyzed Wacker-type oxidation of 2-vinylnaphthalene (**1**).[a]

2		R^1	R^2	R^3	t [h]	Yield 3 [%]	Yield 4 [%]	Yield 5 [%]	Yield 6 [%]
1	a	Et	Et	Et	6	82	12	–	–
2[b]	a	Et	Et	Et	6	72	9	–	–
3[c]	b	iPr	iPr	iPr	24	0	0	–	–
4[d]	c	TMS	TMS	TMS	6	0	0	–	–
5[e]	d	EtO	EtO	EtO	6	5	traces	–	–[f]
6[g]	d	EtO	EtO	EtO	6	32	4	–	–[f]
7[h]	e	C$_6$H$_5$	H	H	4	48	13	–	–
8	f	C$_6$H$_5$	Me	H	6	50	14	80 (R^3=OEt)	–(R^3=OEt) [f]
9	g	C$_6$H$_5$	C$_6$H$_5$	H	6	60	13	73 (R^3=OEt)	7 (R^3=OEt)
10	h	C$_6$H$_5$	Me	Me	2	62	10	73	6
11	i	3,5-(CF$_3$)$_2$C$_6$H$_3$	Me	Me	1.5	74	7	26	–[f]
12	j	C$_6$H$_5$	C$_6$H$_5$	Me	4	75	12	81	9
13	k	C$_6$H$_5$	C$_6$H$_5$	C$_6$H$_5$	2.5	85	12	95	2
14[i]	k	C$_6$H$_5$	C$_6$H$_5$	C$_6$H$_5$	5.5	79	10	76	3
15[b]	k	C$_6$H$_5$	C$_6$H$_5$	C$_6$H$_5$	2.5	55	9	100	0
16[j]	k	C$_6$H$_5$	C$_6$H$_5$	C$_6$H$_5$	2.5	85	11	98	2
17[k]	k	C$_6$H$_5$	C$_6$H$_5$	C$_6$H$_5$	2.5	83	11	100	0

[a] Reaction conditions: **1** (0.65 mmol), FePcF$_{16}$ (5 mol%), hydrosilane **2** (2.0 equiv), EtOH (10 mL), O$_2$ (1 atm), room temperature; yields refer to isolated products; yields of ethoxysilane **5** and silanol **6** are based on the hydrosilane **2**. [b] Reaction under air. [c] After 6 h at room temperature and additional 18 h at reflux temperature, 2-vinylnaphthalene (**1**) was completely recovered. [d] 81% of 2-vinylnaphthalene (**1**) were recovered. [e] 94% of 2-vinylnaphthalene (**1**) were recovered. [f] Detected by MS. [g] Reaction at 70 °C; 41% of 2-vinylnaphthalene (**1**) were recovered. [h] 2,3-Di(naphth-2-yl)butane (11%) and traces of di(1-(naphth-2-yl)eth-1-yl) ether formed as by-products. [i] Reaction with 2.5 mol% of FePcF$_{16}$. [j] Reaction with 1.5 equiv. triphenylsilane (**2k**). [k] Reaction with 1.2 equiv. triphenylsilane (**2k**).
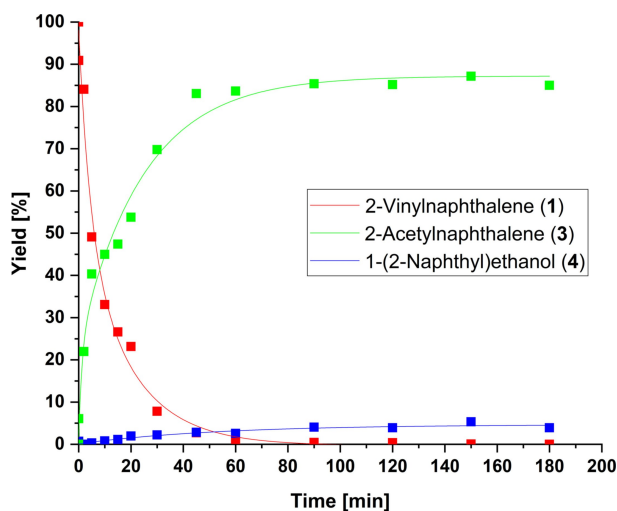
Chemistry–A European Journal

Full Paper
doi.org/10.1002/chem.202102848

Chemistry Europe
European Chemical
Societies Publishing

Figure 1. Course of the oxidation of 2-vinylnaphthalene (**1**) in the presence of FePcF$_{16}$ (5 mol%), Ph$_3$SiH (**2k**; 2 equiv), and O$_2$ (Table 1, entry 13) monitored by GC-MS analysis with naphthalene as internal standard.
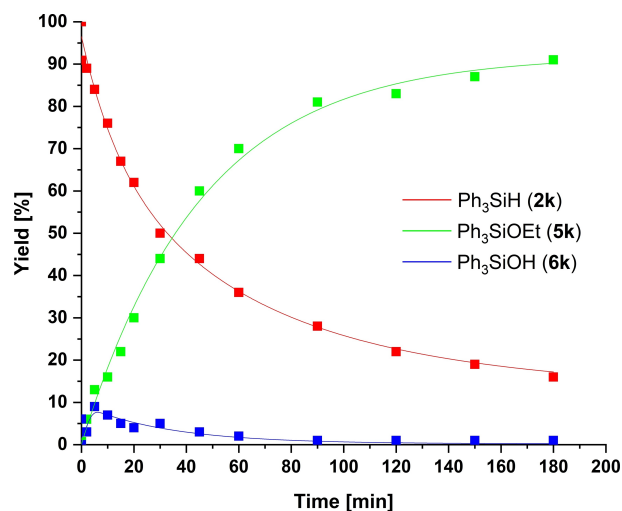

Figure 2. Consumption of triphenylsilane (**2k**) and formation of **5k** and **6k** during the oxidation of 2-vinylnaphthalene (**1**) in the presence of FePcF$_{16}$ (5 mol%), Ph$_3$SiH (**2k**) (2 equiv), and O$_2$ (Table 1, entry 13) monitored by GC-MS analysis with naphthalene as internal standard.

pyrano[3,2-*a*]carbazole alkaloid euchrestifoline.[18] When triphenylsilane (**2k**) was applied, triphenylethoxysilane (**5k**) and small amounts of triphenylsilanol (**6k**) were isolated as by-products. Reducing the amount of catalyst by half (2.5 mol% of FePcF$_{16}$) leads to significantly longer reaction times (Table 1, entry 14). If the reaction is performed under air instead of an oxygen atmosphere, triethylsilane as reductive additive affords better results than triphenylsilane (compare Table 1, entries 2 and 15).

The rate for the transformation of 2-vinylnaphthalene (**1**) into 2-acetylnaphthalene (**3**) and 1-(2-naphthyl)ethanol (**4**) using triphenylsilane (**2k**) was monitored by GC-MS analysis (Figure 1). Using our standard reaction conditions with 2 equivalents of Ph$_3$SiH (**2k**), we observed an immediate consumption of the olefin **1** and the formation of ketone **3** as well as the alcohol **4**. However, the formation of the alcohol **4** is progressing much more slowly in comparison to the ketone **3**. The catalysis using the iron complex FePcF$_{16}$ obviously requires no induction period.

Monitoring the consumption of triphenylsilane (**2k**) by GC-MS analysis (Figure 2) confirmed that about 20% of **2k** were still present even after 3 h, whereas the oxidation of **1** was essentially completed after 1.5 h (compare Figure 1). Thus, using only 1.5 or even 1.2 equivalents of triphenylsilane (**2k**) for the Wacker-type oxidation of **1** provides similar results as with 2 equivalents of **2k** (compare Table 1, entries 13, 16, and 17). Moreover, the time-dependent course for the formation of the triphenylsiloxy by-products shows a steady increase of triphenylethoxysilane (**5k**), whereas the concentration of triphenylsilanol (**6k**) is reaching a maximum after about 5 minutes and then continuously decreases (Figure 2). An explanation for this interesting observation is given along with the detailed mechanism we have proposed for the catalytic cycle (Scheme 3, below).

Previously, we have suggested an in situ generation of the oxygen-bridged complex μ-oxo-bis

[(hexadecafluorophthalocyanine)iron(III)] (O[FePcF$_{16}$]$_2$) during the catalysis by an oxygen reduction process.[12] Formation and applications of μ-oxo-bridged bis(phthalocyanine–iron[III]) complexes were reported previously.[19,20] The electron-deficient complex FePcF$_{16}$ is easily oxidized in solution.[21] Thus, we have prepared the μ-oxo-bridged complex O(FePcF$_{16}$)$_2$ by stirring FePcF$_{16}$ in a 1:1 mixture of toluene and THF at room temperature under an atmosphere of oxygen (Scheme 2),[12,19q] following conditions previously applied to the synthesis of μ-oxo-bridged porphyrin complexes.[22] Electrospray ionization mass-spectrometry (ESI-MS, +10 V) confirmed the structure of O(FePcF$_{16}$)$_2$ by a strong molecular peak at *m/z* 1729.0 for [M+H]$^+$ (Figure S1 in the Supporting Information). Moreover, FePcF$_{16}$ and the μ-oxo-bridged complex O(FePcF$_{16}$)$_2$ exhibit differences in their UV-Vis absorption spectra (Figures S2 and S3, Table S1).

Next, we investigated the Wacker-type oxidation of 2-vinylnaphthalene (**1**) using μ-oxo-bis[(hexadecafluorophthalocyanine)iron(III)] (O[FePcF$_{16}$]$_2$) as catalyst under standard reaction conditions with either triethyl- or
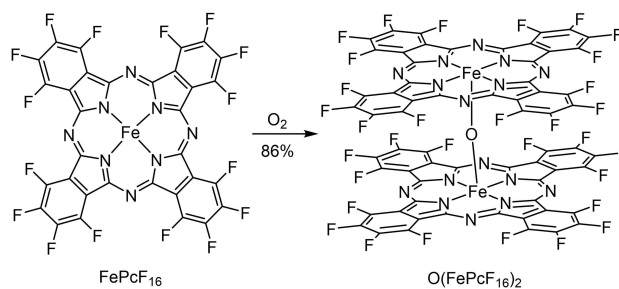
Scheme 2. Synthesis of μ-oxo-bis[(hexadecafluorophthalocyanine)iron(III)] (O[FePcF$_{16}$]$_2$). Reaction conditions: Toluene/THF (1:1), oxygen, room temperature, 1.5 h (86%).

Chem. Eur. J. **2021**, *27*, 16776–16787   www.chemeurj.org

16778

© 2021 The Authors. Chemistry - A European Journal published by Wiley-VCH GmbH

Chemistry–A European Journal

Full Paper
doi.org/10.1002/chem.202102848

Chemistry Europe
European Chemical
Societies Publishing

triphenylsilane as reductive additive (Table 2). The ketone **3** and the alcohol **4** were obtained in the same yields as previously when using FePcF$_{16}$ as catalyst (compare Table 1, entries 1 and 13). This result suggests that the initial step of the FePcF$_{16}$-catalyzed Wacker-type oxidation is the generation of O(FePcF$_{16}$)$_2$.

Using Mössbauer spectroscopy, we have investigated the complexes μ-oxo-bis[(hexadecafluorophthalocyanine)iron(III)] (O[FePcF$_{16}$]$_2$) and hexadecafluorophthalocyanine–iron(II) (FePcF$_{16}$) in solid form as well as in frozen ethanol solution in order to enable their identification in the reaction mixture. Figure 3 shows the Mössbauer spectra of solid O(FePcF$_{16}$)$_2$ (a and c) and FePcF$_{16}$ (b and d) at room temperature (a and b) and at 90.5 K (c and d). The complex O(FePcF$_{16}$)$_2$ shows temperature-dependent Mössbauer spectra (Figure S16). The spectra of solid O(FePcF$_{16}$)$_2$ at 295 and 90.5 K exhibit two iron signals, both having quadrupole splitting with a larger value for signal 1 as compared to signal 2 (Figure 3a and c, Table 3). With decreasing temperature, the proportion of signal 1 increases, whereas the proportion of signal 2 decreases. After warming up the sample to 295 K, the spectrum at this temperature can be reproduced. In a linear μ-oxo-bridged complex O(FePcF$_{16}$)$_2$, both iron atoms have the same chemical environment and thus, only one iron signal would be expected for the Mössbauer spectrum. However, two iron signals are observed. The second signal most likely derives from the bent form of O(FePcF$_{16}$)$_2$ (Figure S17). Magnetic susceptibility measurements confirmed a linear relationship between the inverse magnetic susceptibility and the temperature in the range of 15 to 299 K which was investigated by Mössbauer spectroscopy (Figure 4). Thus, a spin cross-over process can be ruled out. The large temperature dependence of the proportions of signals 1 and 2 indicates a reversible structural transition from a linear to a bent form.[19r] For the Mössbauer spectra of solid FePcF$_{16}$ (Figure 3b and d), only one signal is expected. However, three signals are exhibited in the corresponding spectra.[23] The first two signals have parameters in agreement with those of O(FePcF$_{16}$)$_2$ (Table 3). The major differences are that the first signal has a consistently larger isomer shift of about 0.1 mm s^{-1} for FePcF$_{16}$, ≈0.2 mm s^{-1} for FePcF$_{16}$ at room temperature and ≈0.1 mm s^{-1} for O(FePcF$_{16}$)$_2$. Additionally, the quadrupole splitting of signal 2 is ≈15–40% larger for FePcF$_{16}$. The qualitative temperature

Table 2. O(FePcF$_{16}$)$_2$-catalyzed Wacker-type oxidation of 2-vinylnaphthalene (**1**).[a]

	R$_3$SiH (**2**)	t [h]	Yield **3** [%]	Yield **4** [%]
1	Et$_3$SiH (**2a**)	10	84	13
2[b]	Et$_3$SiH (**2a**)	4	84	12
3[c]	Ph$_3$SiH (**2k**)	4	85	12

[a] Reaction conditions: **1** (0.65 mmol), O(FePcF$_{16}$)$_2$ (2.5 mol%), hydrosilane **2** (2 equiv), EtOH (10 mL), O$_2$ (1 atm), room temperature; yields refer to isolated products. [b] 5 mol% of O(FePcF$_{16}$)$_2$. [c] Ph$_3$SiOEt (**5k**) was isolated in 95% yield, Ph$_3$SiOH (**6k**) was isolated in 2% yield based on Ph$_3$SiH (**2k**).
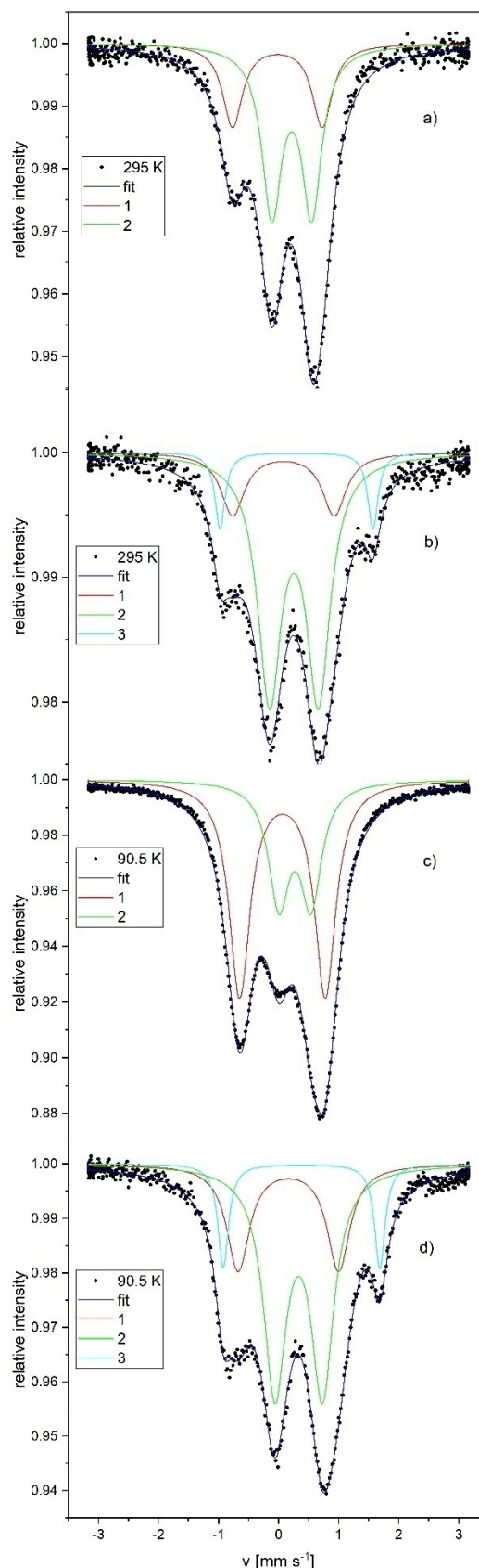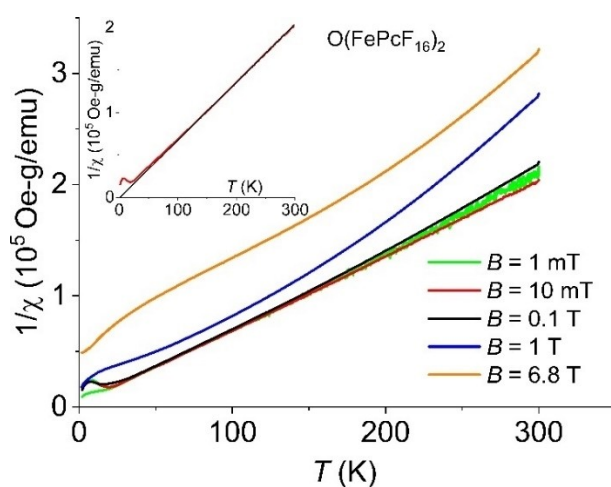

Figure 3. Mössbauer spectra of a) solid O(FePcF$_{16}$)$_2$ and b) solid FePcF$_{16}$ at room temperature and of c) solid O(FePcF$_{16}$)$_2$ and d) solid FePcF$_{16}$ at 90.5 K. Experimental data are shown as black dots along with the overall fit (dark blue line). Contributions are shown in color as upper traces. Parameters: see Table 3.

Chemistry–A European Journal

Full Paper
doi.org/10.1002/chem.202102848

Chemistry Europe
European Chemical
Societies Publishing

Table 3. Parameters for the iron complexes $O(FePcF_{16})_2$ and $FePcF_{16}$ determined from simulations of the Mössbauer spectra shown in Figures 3 and 5.

Compound	Site	δ [mm s^{-1}]	ΔE_Q [mm s^{-1}]	Rel. area [%]
$O(FePcF_{16})_2$ 295 K	1	1.493(8)	0.092(14)	33
	2	0.665(2)	0.330(14)	67
$FePcF_{16}$ 295 K	1	1.691(20)	0.192(20)	20
	2	0.817(7)	0.367(13)	71
	3	2.546(12)	0.409(16)	9
$O(FePcF_{16})_2$ 90.5 K	1	1.427(4)	0.175(15)	64
	2	0.551(4)	0.383(10)	36
$FePcF_{16}$ 90.5 K	1	1.672(8)	0.274(13)	28
	2	0.762(4)	0.445(12)	59
	3	2.606(5)	0.492(13)	13
$O(FePcF_{16})_2$ ethanol, 77 K	1	1.580(10)	0.095(12)	65
	2	0.469(25)	0.332(11)	35
$FePcF_{16}$ ethanol, 90.5 K	1	1.519(5)	0.248(13)	42
	2	0.665(4)	0.448(12)	53
	3	2.530(33)	0.449(25)	5

Figure 4. Inverse magnetic susceptibility of the μ-oxo-bridged iron complex $O(FePcF_{16})_2$ dependent on the temperature at different magnetic fields.

dependence for the Mössbauer spectra of $O(FePcF_{16})_2$ and $FePcF_{16}$ is identical, with signal 1 increasing and signal 2 decreasing in intensity when decreasing the temperature. The results described above indicate that the sample of $FePcF_{16}$ was already partly oxidized to $O(FePcF_{16})_2$, thus giving rise to signals 1 and 2. The deviations for the signals 1 and 2 between the spectra of $O(FePcF_{16})_2$ and $FePcF_{16}$ are tentatively ascribed to $FePcF_{16}/O(FePcF_{16})_2$ interactions. Similar observations have been reported for the Mössbauer spectrum of FePc.[24] The third signal in the Mössbauer spectrum of $FePcF_{16}$ has parameters similar to those of FePc and thus is assigned to $FePcF_{16}$.[25] The isomer shift of 0.202(18) mm s^{-1} is larger than in FePc, indicating a lower electron density due to the electron withdrawing effect of the fluorine atoms.[21] The quadrupole splitting in the Mössbauer spectrum of $FePcF_{16}$ shows no significant deviation from FePc, indicating that the electron withdrawal is limited, since (FePc)$^+$ is reported to have a considerably larger quadrupole splitting.[25c] This observation combined with the isomer
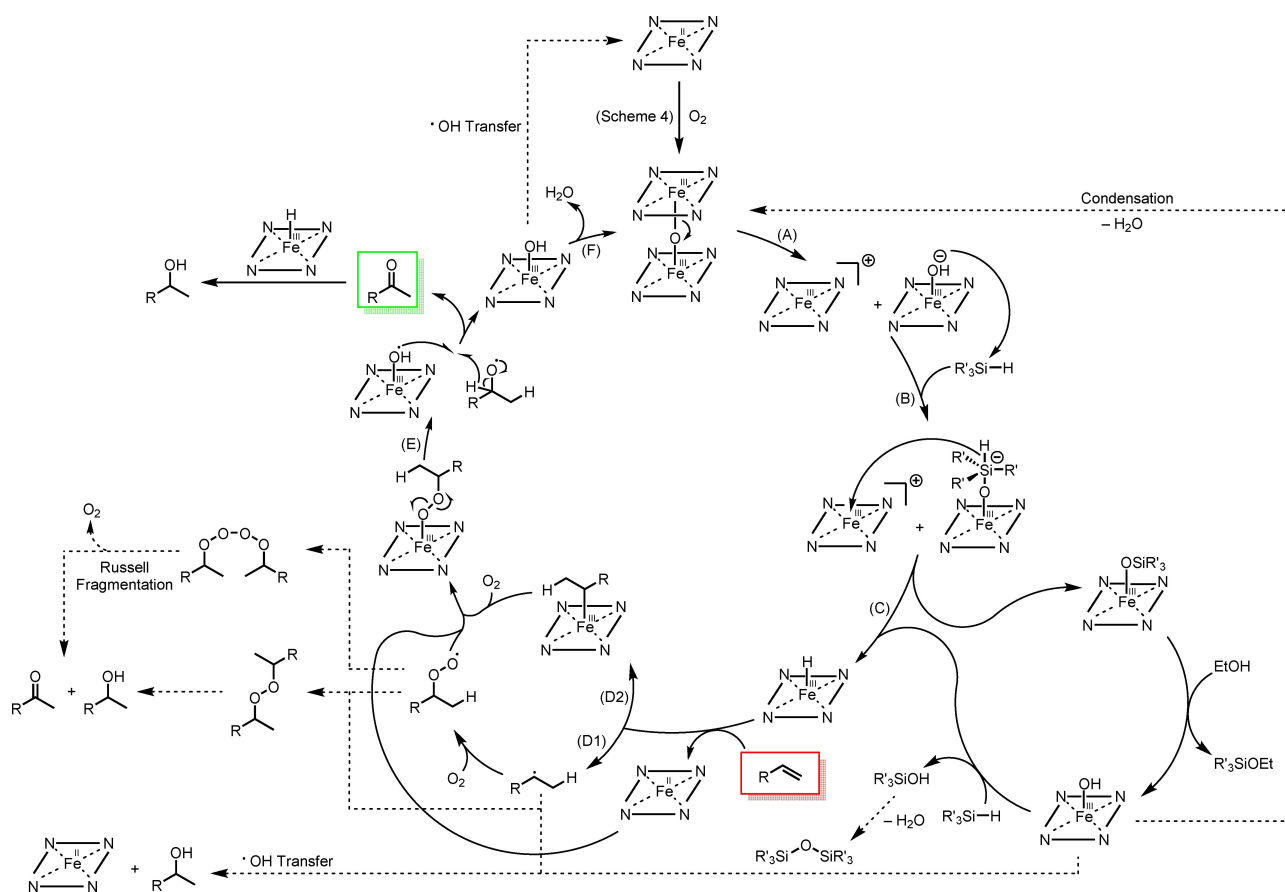
shift of $\delta = 0.409(16)$ mm s^{-1} indicates that iron is in the oxidation state of $+$II (low spin).

Moreover, we have investigated frozen ethanol solutions of $O(FePcF_{16})_2$ and $FePcF_{16}$ by Mössbauer spectroscopy (Figure 5). Also in these spectra, two signals are exhibited by $O(FePcF_{16})_2$ and three signals by $FePcF_{16}$. Thus, the spectra of the complexes in ethanolic solution are very similar to those of the corresponding powders. Most significantly the three signals differ for $FePcF_{16}$, with the second and third signal loosing intensity, while the first signal increases. The main quantitative differences for $O(FePcF_{16})_2$ are the about 0.1 mm s^{-1} higher isomer shift of the first signal and the about 25% smaller ΔE_Q component for the second signal as well as variations in the signal proportions for $FePcF_{16}$ solution. These changes are most likely caused by interactions with ethanol.

Mössbauer spectroscopic investigations of frozen solutions of the reaction mixture confirmed the presence of $FePcF_{16}$, $O(FePcF_{16})_2$, and of an additional iron(II) complex which could not be assigned (Figure S18).

Based on the present experimental findings and earlier studies,[12,14] we have proposed a detailed mechanism for the catalytic cycle of the $FePcF_{16}$-catalyzed oxidation of olefins to ketones using triethyl- or triphenylsilane (**2a** or **2k**) as reductive additive and molecular oxygen as sole oxidant (Scheme 3).
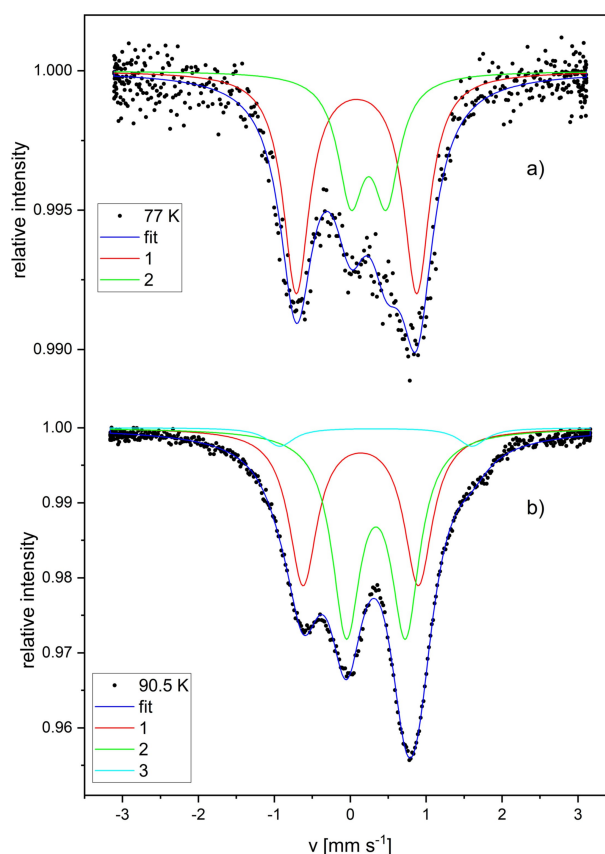
Figure 5. Mössbauer spectrum of a) the μ-oxo-bridged iron complex $O(FePcF_{16})_2$ and b) $FePcF_{16}$ in frozen ethanol solutions. Experimental data are shown as black dots along with the overall fit (dark blue lines). Contributions are shown in color as upper traces. Parameters: see Table 3.

Chemistry–A European Journal

Full Paper
doi.org/10.1002/chem.202102848

Chemistry Europe
European Chemical
Societies Publishing

Scheme 3. Detailed mechanism for the FePcF$_{16}$-catalyzed Wacker-type oxidation of olefins to ketones (simplified representation of the hexadecafluorophthalo-cyanine ligand for clarity; possible axially bound neutral ligands (e.g., EtOH) are not shown; presumed side reactions as dashed lines). R = aryl, alkyl; R' = Et, Ph.

Initially, the hexadecafluorophthalocyanine–iron(II) complex (FePcF$_{16}$) is oxidized by molecular oxygen to the oxygen-bridged complex μ-oxo-bis[(hexadecafluorophthalocyanine)iron (III)] (O[FePcF$_{16}$]$_2$) (Scheme 2). This hypothesis is supported by the fact that both complexes, FePcF$_{16}$ and O(FePcF$_{16}$)$_2$, provide identical results when applied as catalysts in this process (compare Table 1, entries 1 and 13, with Table 2). The concomitant oxygen reduction is believed to proceed according to a similar mechanism as proposed previously for the formation of related μ-oxo-bis[(phthalocyanine)iron(III)] and μ-oxo-bis[(porphyrin)iron(III)] complexes (Scheme 4).[19,20,26,27a] Subsequent dissociation of the μ-oxo-bridged diiron complex O(FePcF$_{16}$)$_2$ generates a cationic iron fragment and an anionic oxido–iron complex (A).[27] This fragmentation was supported by an ESI-MS (−100 V) from the crude reaction mixture of the FePcF$_{16}$-catalyzed oxidation of **1** (Table 1, entry 13), which exhibited a peak at *m/z* 871.7 corresponding to [OFePcF$_{16}$]$^-$. Nucleophilic attack of the anionic oxido–iron complex at the silicon atom of the silane provides an intermediate pentavalent silicon anion (B). Subsequent hydride transfer to the cationic iron species leads to a hydrido–iron(III) complex (C).[2e,28,29] The formation of the hydrido–iron(III) complex appears to be involved in the rate-determining step of this catalysis as confirmed by the strong dependence of the reaction rate on the concentration of
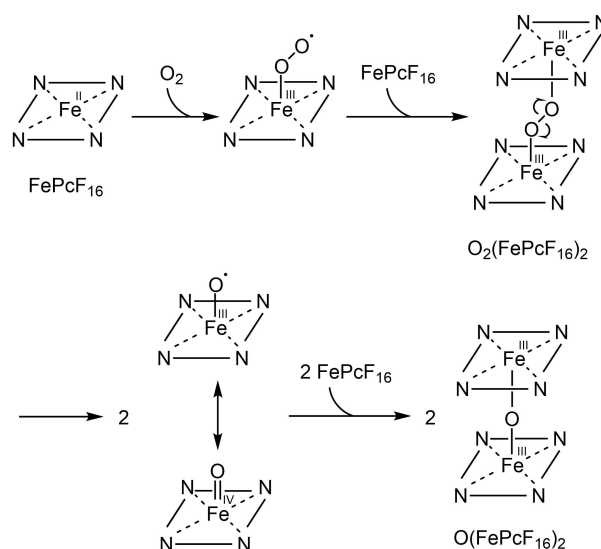
Scheme 4. Reduction of oxygen by oxidation of iron(II) to iron(III) for the hexadecafluorophthalocyanine–iron(II) complex FePcF$_{16}$ (simplified representation of the hexadecafluorophthalocyanine ligand for clarity).
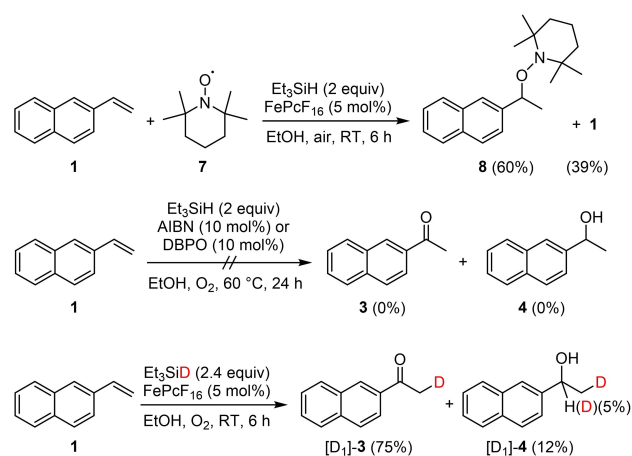
the catalyst (compare entries 13 and 14 in Table 1, and entries 1 and 2 in Table 2). The resulting siloxy–iron(III) complex is

Chemistry–A European Journal

Full Paper
doi.org/10.1002/chem.202102848

Chemistry Europe
European Chemical
Societies Publishing

attacked by ethanol to form the ethoxysilane R'$_3$SiOEt (**5**) and a hydroxy–iron(III) complex which has been identified by ESI-MS ($+75$ V; m/z 873.1) in the reaction mixture of the oxidation of **1**. For triphenylethoxysilane (**5k**), the proposed route for the formation of the ethoxysilane has been supported by several mechanistic experiments (Scheme 5). When stirred in ethanol at room temperature, neither triphenylsilane (**2k**) nor triphenylsilanol (**6k**) afforded triphenylethoxysilane (**5k**; Figures S7 and S8). Thus, a simple ethanolysis can be excluded for both compounds. However, stirring an ethanolic solution of triphenylsilane (**2k**) in the presence of catalytic amounts of either FePcF$_{16}$ or O(FePcF$_{16}$)$_2$ leads to the formation of significant amounts triphenylethoxysilane (**5k**) along with traces of triphenylsilanol (**6k**) which could be detected by GC-MS analysis (Figures S9 and S10). Therefore, the excess of triphenylsilane (**2k**) is converted into triphenylethoxysilane (**5k**) under the reaction conditions used for the catalysis (compare Figure 2). In agreement with this conclusion, the decrease of the amount of reductive additive from 2.0 equivalents of **2k** to 1.5 or 1.2 equivalents of **2k** provided the same result for the FePcF$_{16}$-catalyzed Wacker-type oxidation (Table 1, entries 13, 16, and 17). The stoichiometric reaction of **2k** with 1 equivalent of O(FePcF$_{16}$)$_2$ under an atmosphere of argon provides **5k** and **6k** and confirms that this transformation occurs in the absence of O$_2$. A transformation of triphenylsilanol (**6k**) into triphenylethoxysilane (**5k**) with ethanol in the presence of FePcF$_{16}$ or O(FePcF$_{16}$)$_2$ is not possible (Figures S11 and S12). Thus, the decrease of the concentration of triphenylsilanol (**6k**) observed during the reaction after the initial increase (Figure 2) is ascribed to the formation of siloxane by condensation.[30] Using deuterated ethanol (C$_2$D$_5$OD; 99% D content) as solvent for the FePcF$_{16}$-catalyzed Wacker-type oxidation of **1** led to no
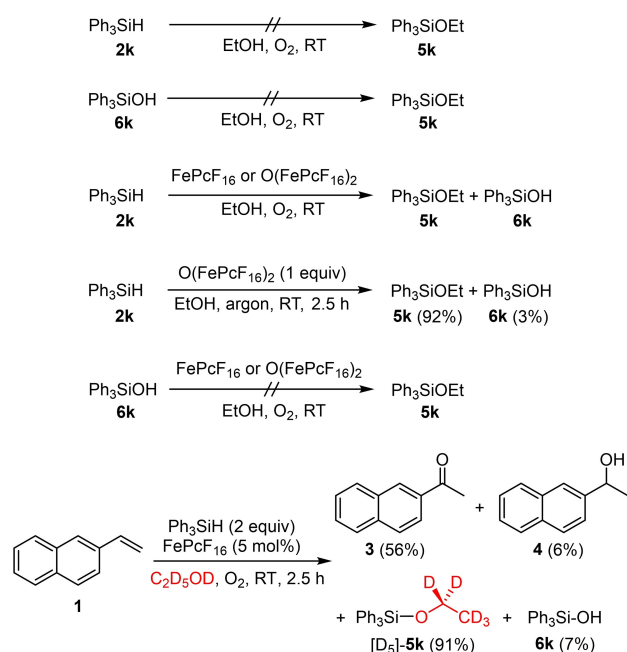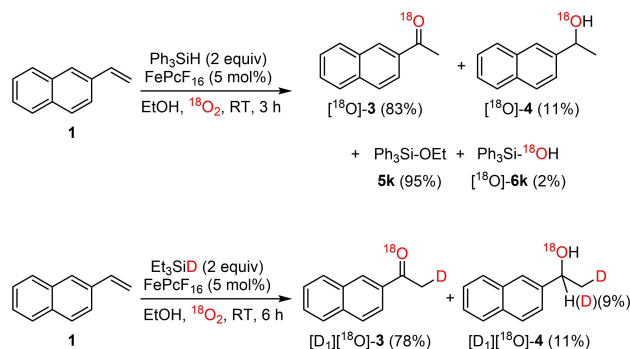
deuterium incorporation into the ketone **3** and the alcohol **4**, but a deuterated triphenylethoxysilane [D$_5$]-**5** could be isolated (Scheme 5). This result indicates that the ethoxy group of **5** originates from the solvent (ethanol). The formation of minor amounts of silanol R'$_3$SiOH (**6**) is explained by reaction of hydrosilane with the hydroxy–iron(III) complex which provides an alternative pathway to the hydrido–iron(III) complex. This mechanism for the formation of the silanol R'$_3$SiOH (**6**) derives support from the fact that in contrast to the oxygen atom of the ethoxysilane **5**, the oxygen atom of **6** originates from the oxygen atmosphere (see the ^{18}O-labeling experiment in Scheme 7, below). The hydrido–iron(III) complex opens up two different mechanistic pathways generating either an alkyl radical by hydrogen atom transfer (HAT)[2e,29,31] to the olefin (Scheme 3, path D1)[32] or a (1-methylalkyl)–iron(III) complex by hydrometalation (path D2).[33] By addition of (2,2,6,6-tetramethylpiperidin-1-yl)oxyl (TEMPO; **7**), the intermediate radical proposed for path D1 could be intercepted to give compound **8** with complete inhibition of ketone formation (Scheme 6). The radical scavenger galvinoxyl (4-[(3,5-di-*tert*-butyl-4-oxocyclohexa-2,5-dien-1-ylidene)methyl]-2,6-di-*tert*-butylphenoxyl) also inhibited the reaction and only starting material **1** was recovered. Using radical starters like azobis(isobutyronitrile) (AIBN) or dibenzoyl peroxide (DBPO) instead of the iron complex gave no conversion of **1**, indicating that the iron complex does not just function as a simple radical starter. The HAT mechanism was supported by using Et$_3$SiD (98% D content) as the reductive additive for the iron-catalyzed Wacker-type oxidation of **1** which resulted in 98% deuterium incorporation at the methyl groups of ketone **3** and alcohol **4** (Scheme 6). In this experiment, an additional deuterium incorporation of about 5% could be detected at the α-hydroxy position of [D$_1$]-**4** (GC-MS, ^{1}H NMR). In conclusion, it is evident that only a very minor amount of the alcohol **4** results from a subsequent iron-catalyzed reduction of ketone **3** (see below). The pathways D1 and D2 would ultimately both lead to the same alkylperoxy–iron(III) complex. Reaction of the radical with

Scheme 5. Mechanistic experiments supporting the proposed route for the formation of triphenylethoxysilane (**5k**).

Scheme 6. Mechanistic experiments supporting the iron-catalyzed HAT. According to ^{1}H NMR: 98% deuterium incorporation in the methyl groups of **3** and **4**. AIBN = azobisisobutyronitrile, DBPO = dibenzoyl peroxide.

Chemistry–A European Journal

Full Paper
doi.org/10.1002/chem.202102848

Chemistry Europe
European Chemical
Societies Publishing

Scheme 7. Mechanistic experiments confirming the origin of the oxygen and hydrogen atoms in the products of the iron-catalyzed Wacker-type oxidation. Equation (1): According to GC-MS: 95% ^{18}O incorporation in **3**, **4**, and **6k**. Equation (2): According to ^1H NMR: 98% deuterium incorporation in the methyl group of **3** and according to GC-MS: 90% ^{18}O incorporation in **3** and 88% ^{18}O incorporation in **4**.

molecular oxygen to a peroxy radical followed by coordination to the iron(II) complex gives the alkylperoxy–iron(III) complex (D1).[32] Alternatively, this intermediate is generated by insertion of dioxygen into the (1-methylalkyl)–iron(III) complex (D2).[33a,34] Homolytic cleavage of the O−O bond generates two radical species (E).[26d,35] Subsequent abstraction of a hydrogen atom leads to the ketone and a hydroxy–iron(III) complex.[33a] Condensation of two hydroxy–iron(III) complexes regenerates the μ-oxo-bridged diiron complex $O(FePcF_{16})_2$ and thus completes the catalytic cycle (F).[27a,34]
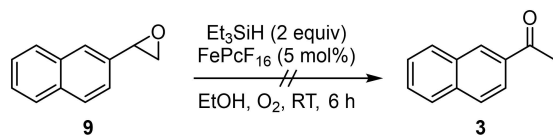
Additional strong support for the proposed mechanism depicted in Scheme 3 derives from further isotopic labeling studies. Previously, we have shown that no product is formed when the $FePcF_{16}$-catalyzed Wacker-type oxidation of **1** is performed under an argon atmosphere.[12] In order to demonstrate the origin of the incorporated oxygen atom, we have executed this transformation under an atmosphere of $^{18}O_2$ ($^{18}O_2$ isotope purity: > 97.17%) using otherwise identical conditions (Scheme 7). In fact, an ^{18}O incorporation of 95% as detected by EI-MS for the ketone [^{18}O]-**3** and for the alcohol [^{18}O]-**4** unequivocally confirmed that the oxygen atoms of both products derive from the atmosphere. It is noteworthy that a complete ^{18}O incorporation (95% detected by EI-MS) was also found for the silanol [^{18}O]-**6k** but no ^{18}O was present in the ethoxysilane **5k**. Combined with the experiments shown in Scheme 5, this observation provides clear evidence for the origin of the silyl compounds **5** and **6** as outlined in Scheme 3. Finally, a combined labeling experiment for the $FePcF_{16}$-catalyzed Wacker-type oxidation of **1** using Et_3SiD (98% D content) as reductive additive under an atmosphere of $^{18}O_2$ ($^{18}O_2$ isotope purity: > 97.17%) in dry and degassed ethanol afforded the ketone [D_1][^{18}O]-**3** and the alcohol [D_1][^{18}O]-**4** (Scheme 7). For the alcohol [D_1]-**4** an additional deuterium incorporation of about 9% could be detected at the α-hydroxy position. An ESI-MS (+50 V) of the reaction mixture showed a peak at *m/z* 1731.0 for the mass of the ^{18}O-labeled μ-oxo-bis [(hexadecafluorophthalocyanine)iron(III)] complex ($^{18}O[FePcF_{16}]_2$). Thus, the ^{18}O incorporation could be also

demonstrated for the μ-oxo-bridged complex which confirms the catalytic cycle depicted in Scheme 3.

Four different mechanisms may be considered for the formation of alcohol in the $FePcF_{16}$-catalyzed Wacker-type oxidation (cf. Scheme 3). We assume that the alcohol as by-product most likely is generated by an OH transfer process from the hydroxy–iron(III) complex to the intermediate radical, similar to the rebound mechanism described by Goldberg and co-workers.[36] In agreement with this hypothesis, the α-hydrogen atom of 2-vinylnaphthalene (**1**) should be retained in the molecule during the transformation into the alcohol **4**. In fact, using the α-deuterated 2-vinylnaphthalene ([α-D_1]-**1**; 88% D content) as starting material, the corresponding alcohol ([α-D_1]-**4**) deuterated at the benzylic position (85% D content) was obtained as by-product of the transformation (Scheme 8). Alternatively, this outcome could be also explained by formation of a peroxide and subsequent iron-catalyzed conversion to ketone and alcohol,[37] or by peroxyradical dimerization to a tetroxide followed by Russell fragmentation with concomitant loss of oxygen.[38] Following the two latter pathways, the α-hydrogen atom of the olefin would remain in the alcohol, however, both of them would deliver the ketone and the alcohol in an equimolar ratio. The fourth pathway for the formation of alcohol is the iron-catalyzed reduction of the generated ketone. The experiments using Et_3SiD as reductive additive have already indicated this route by the partial deuteration (5–9%) at the benzylic position (Schemes 6 and 7). For a direct confirmation, 2-acetylnaphthalene (**3**) was stirred under standard reaction conditions with Et_3SiD (98% D content) as reductive additive and $FePcF_{16}$ as catalyst to afford the alcohol [α-D_1]-**4** in 4% yield with a deuterium incorporation of 98% at the benzylic position (Scheme 8). This subsequent reduction of ketone **3** diminishes the deuterium content observed at the benzylic position of the alcohol **4** in the experiment described in equation 1 of Scheme 8. In conclusion, the $FePcF_{16}$-catalyzed Wacker-type oxidation of 2-vinylnaphthalene (**1**) provides the alcohol **4** in about 11–12% yield (Table 1, entries 1 and 13; Schemes 6 and 7). To this amount of the by-product **4**, the iron-catalyzed reduction of 2-acetylnaphthalene (**3**) contributes a maximum of 1% yield as deduced from the partial deuteration of 5–9% at the benzylic position when using Et_3SiD as reductive additive (Schemes 6 and 7). The major
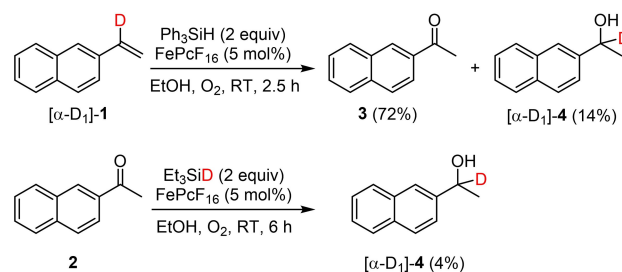
Scheme 8. Experiments demonstrating the two different mechanisms leading to the alcohol by-product of the iron-catalyzed Wacker-type oxidation. Equation (1): According to ^1H NMR: 85% deuterium incorporation at the benzylic position of **4**. Equation (2): According to ^1H NMR: 98% deuterium incorporation at the benzylic position of **4**.

Chemistry–A European Journal

Full Paper
doi.org/10.1002/chem.202102848

Chemistry Europe
European Chemical
Societies Publishing

Scheme 9. Attempted Meinwald rearrangement of the epoxide **9**.

amount of alcohol **4** is most likely formed by an OH radical transfer from the intermediate hydroxy–iron(III) complex to the radical generated by HAT.

The isotopic labeling studies using Et_3SiD and $^{18}O_2$ strongly support our proposed mechanism and confirm the origin of the oxygen and hydrogen atoms (Scheme 3). However, as porphyrin–iron and phthalocyanine–iron complexes are known to catalyze the oxidation of alkenes to epoxides,[20k,39] an alternative pathway via an iron-catalyzed epoxidation followed by Meinwald rearrangement[40] might still at least partially be involved in the formation of ketone **3**. To rule out this possibility, we converted 2-vinylnaphthalene (**1**) into the corresponding epoxide **9** following a literature procedure[41] and submitted it to the standard reaction conditions for the $FePcF_{16}$-catalyzed Wacker-type oxidation (Scheme 9). However, neither the ketone **3** nor the alcohol **4** were formed and only 39% of the starting material **9** could be re-isolated, indicating a large degree of decomposition. Therefore, a reaction pathway to the ketone **3** via epoxide formation and subsequent Meinwald rearrangement does not play any role in the present process.

Conclusion

In this work, we have studied in detail the mechanism of our $FePcF_{16}$-catalyzed Wacker-type oxidation in ethanol by using 2-vinylnaphthalene as model compound. In the initial step, the iron(II) complex $FePcF_{16}$ was oxidized by molecular oxygen to the μ-oxo-bridged diiron(III) complex $O(FePcF_{16})_2$. Mössbauer spectroscopy and additional magnetic susceptibility measurements of $O(FePcF_{16})_2$ suggested that this complex exists in two forms with either a linear or a bent arrangement of the hexadecafluorophthalocyanine ligands. Triethyl- or triphenylsilane as reductive additive generate an intermediate hydrido–iron(III) complex that, by sequential reaction with the olefin and molecular oxygen, leads to an alkylperoxy–iron(III) complex. Homolytic fragmentation of the latter ultimately affords the ketone and a hydroxy–iron(III) complex that regenerates $O(FePcF_{16})_2$ by condensation. The alcohol by-product is thought to be formed primarily by an OH radical transfer from the hydroxy–iron(III) complex to an intermediate alkyl radical, and only to a small extent by a $FePcF_{16}$-catalyzed reduction of the ketone. The mechanism for the $FePcF_{16}$-catalyzed Wacker-type oxidation described above was confirmed by isotopic labeling experiments (with C_2D_5OD, Et_3SiD, and $^{18}O_2$); this enabled the rationalization of a variety of experimental observations related to the $FePcF_{16}$-catalyzed oxidation of olefins to ketones. The nearly complete picture of the reaction mechanism presented

herein should be highly useful for further optimization of this process by variation of the reaction parameters and modification of the catalyst.

Experimental Section

General methods: All reactions were carried out in oven-dried glassware under 1 atm of oxygen using a balloon unless otherwise notified. Reagents and solvents were received from commercial suppliers (TCI, Sigma-Aldrich, Alfa Aesar) and used without further purification, unless otherwise stated. Ethanol used as solvent for the iron-catalyzed Wacker-type reaction was purchased from Fisher Scientific or VWR in analytical reagent grade ($\geq$99.8%). $^{18}O_2$ was obtained from Eurisotope ($^{18}O_2$ 97.17%, $^{16}O_2$ 1.93%, $^{17}O_2$ 0.9%; impurities: Ar 25 ppm, H_2 18 ppm, $N_2 < 2000$ ppm, $^4He < 1000$ ppm; analytical method: ICP-MS). Dichloromethane, diethyl ether, toluene, THF and benzene were dried using a solvent purification system (MBraun-SPS). Automated flash chromatography was performed on a Büchi Sepacore system (precolumn: Ø 2 cm, length 10 cm; separation column: Ø 2 cm, length 20 cm; flow rate: 14 mL min^{-1}; maximal working pressure: 10 bar) equipped with an UV monitor using silica gel from Acros Organics (0.035–0.070 mm). Thin layer chromatography was performed with TLC plates from Merck (60 F254), using short-wave UV light for visualization or *p*-anisaldehyde solution as developing agent. Melting points were measured on a Gallenkamp MPD 350 melting point apparatus. Ultraviolet spectra were recorded on a Perkin Elmer 25 UV/VIS spectrometer, shoulders are labelled with sh. Fluorescence spectra were measured on a Varian Cary Eclipse spectrophotometer. Infrared spectra were recorded on a Thermo Nicolet Avatar 360 FTIR spectrometer by using the ATR (Attenuated Total Reflectance) method. Wave numbers ν are reported in cm^{-1}. NMR spectra (^1H, ^{13}C and ^{19}F) were recorded on Bruker AC 300, Bruker DRX 500 and Avance III 600 spectrometers. Chemical shifts δ are reported in parts per million (ppm) with the solvent signal as internal standard.[42] ^{19}F spectra were referenced externally to (trifluoromethyl)benzene in $CDCl_3$. Coupling constants J are given in Hertz [Hz]. The following abbreviations have been used to explain NMR peak multiplicities: s = singlet, d = doublet, t = triplet, q = quartet, quin = quintet, sxt = sextet, sept = septet, m = multiplet, br = broad, and combinations of them. EI mass spectra were recorded by GC-MS coupling using an Agilent Technologies 6890 N GC system equipped with a 5973 mass selective detector (electron impact, 70 eV). The GC-MS yields of products and conversions were determined by using naphthalene as the internal standard. ESI mass spectra were recorded on a Bruker Esquire LC with an ion trap detector. Positive and negative ions were detected. HRMS (ESI-TOF) were recorded on a Xevo G2-XS QToF from Waters. Elemental analyses were measured on an EuroVector EuroEA3000 elemental analyzer. The ^{57}Fe-Mössbauer measurements were conducted in a nitrogen shielded Cryo Vac flow cryostat. Measurements have been carried out at temperatures in the range of 15 K to 296 K using liquid nitrogen or liquid helium for cooling. A Rh/Co source driven by a DFG-500 frequency generator in sinusoidal mode was used. The detection device is a proportional counter tube in combination with a CMTE multichannel data processor MCD 301/8 K and a WissEL single channel analyzer Timing SCA to set the energy window. All isomer shifts are stated relative to α-Fe. Data evaluation has been performed using Mössfit.[43]

(1,2,3,4,8,9,10,11,15,16,17,18,22,23,24,25-Hexadecafluorophthalocyaninato)iron(II) ($FePcF_{16}$):[12,13] [CAS 23844-93-1]: A solution of $Fe(CO)_5$ (1.45 g, 7.40 mmol) in 1-methylnaphthalene (20 mL) was slowly added over a period of 1 h to a solution of 3,4,5,6-tetrafluorophthalonitrile (5.03 g, 25.1 mmol) in 1-meth-

Chemistry–A European Journal

Full Paper
doi.org/10.1002/chem.202102848

Chemistry Europe
European Chemical
Societies Publishing

ylnaphthalene (50 mL) under an atmosphere of argon at 220 °C. After the addition was completed, the resulting dark blue solution was stirred at 220 °C for an additional hour. The reaction mixture was allowed to cool to room temperature, benzene (20 mL) was added, and the mixture was filtered over a frit. The residue was washed with benzene (50 mL), acetone (25 mL), and diethyl ether (25 mL) to give the product which was subsequently triturated to a fine powder. The powder was washed with benzene (50 mL), diethyl ether (25 mL), acetone (25 mL), again with benzene (50 mL), and finally dried in high vacuum to afford FePcF$_{16}$ as a dark blue to blackish powder in 69% yield (3.70 g, 4.32 mmol). UV (MeOH): $\lambda =$ 629, 655, 685 (sh) nm (Figure S2); fluorescence (MeOH): $\lambda_{ex} =$ 304 nm, $\lambda_{em} =$ 338, 460 (weak), 656 (weak) nm; IR (ATR) $\nu =$ 2954, 2631, 2440, 2024, 1732, 1643, 1619, 1558, 1522, 1484, 1459, 1395, 1319, 1266, 1130, 1068, 958, 837, 793, 751, 694, 658 cm^{-1}; MS (ESI, + 25 V): m/z 857.2 [M + H]$^+$; MS (ESI, −10 V): m/z 886.8 [M + OMe]$^-$, 914.7 [M + OAc]$^-$; HRMS (ESI) calcd for C$_{32}$HF$_{16}$FeN$_8^+$ ([M + H]$^+$): 856.9413; found: 856.9406; elemental analysis (%) calcd for C$_{32}$F$_{16}$FeN$_8$: C 44.89, N 13.09; found: C 44.54, N 13.03.

The spectroscopic data are in agreement with those reported in the literature.[12,13]

μ-Oxo-bis[(1,2,3,4,8,9,10,11,15,16,17,18,22,23,24,25-hexadeca-fluorophthalocyaninato)iron(III)] (O[FePcF$_{16}$]$_2$): A solution of FePcF$_{16}$ (205 mg, 0.239 mmol) in THF (25 mL) and toluene (25 mL) was vigorously stirred at room temperature under an atmosphere of oxygen for 1.5 h. The reaction mixture was subsequently transferred into a separating funnel with diethyl ether (30 mL), washed with an aqueous solution of NaOH (0.2 M, 2×30 mL), and the aqueous layer was extracted with diethyl ether (7×25 mL). The combined organic layers were dried over magnesium sulfate, filtered, and the solvent was evaporated under reduced pressure. The resulting dark violet crystalline solid was crushed, collected on a Buchner frit, and washed with water (100 mL), a small amount of acetone (10 mL), benzene (20 mL) and finally again with water (50 mL). The resulting solid was dried in high vacuum. The procedure provided O(FePcF$_{16}$)$_2$ as a violet crystalline solid in 86% yield (177 mg, 0.103 mmol). UV (MeOH): $\lambda =$ 622 nm (Figure S3); fluorescence (MeOH): $\lambda_{ex} =$ 310 nm, $\lambda_{em} =$ 366, 467 (weak) nm; IR (ATR) $\nu =$ 2955, 2925, 2850, 2628, 1640, 1613, 1559, 1523, 1485, 1460, 1397, 1319, 1275, 1144, 1073, 1025, 960, 945, 863, 839, 760, 709 cm^{-1}; MS (ESI, + 10 V): m/z 1729.0 [M + H]$^+$ (Figure S1); MS (ESI, −75 V): m/z 1727.8 [M]$^-$; HRMS (ESI) calcd for C$_{64}$HF$_{32}$Fe$_2$N$_{16}$O$^+$ ([M + H]$^+$): 1728.8702; found: 1728.8661.

Procedure for the FePcF$_{16}$-catalyzed Wacker-type oxidation: A solution of 2-vinylnaphthalene (**1**) (101 mg, 0.655 mmol), FePcF$_{16}$ (28.0 mg, 32.7 μmol), and Ph$_3$SiH (**2 k**) (254 mg, 0.975 mmol) in ethanol (10 mL) was vigorously stirred under an atmosphere of oxygen at room temperature for 2.5 h. The crude product was directly adsorbed at silica gel and purified by automated column chromatography (5–22% EtOAc/isohexane, 90 min) to provide 1-(naphthalen-2-yl)ethanone (**3**) (94.9 mg, 0.557 mmol, 85%) as a colorless solid, the alcohol **4** (11.7 mg, 67.9 μmol, 11%) as a colorless solid, triphenylethoxysilane (**5 k**) (294 mg, 0.965 mmol, 98%) as colorless crystals, and triphenylsilanol (**6 k**) (6.4 mg, 2.3 μmol, 2%) as a colorless solid.

Procedure for the O(FePcF$_{16}$)$_2$-catalyzed Wacker-type oxidation: A solution of 2-vinylnaphthalene (**1**) (100 mg, 0.649 mmol), O(FePcF$_{16}$)$_2$ (27.7 mg, 16.0 μmol), and Ph$_3$SiH (**2 k**) (340 mg, 1.30 mmol) in ethanol (10 mL) was vigorously stirred under an atmosphere of oxygen at room temperature for 4 h. The crude product was directly adsorbed at silica gel and purified by automated column chromatography (5–22% EtOAc/isohexane, 90 min) to afford 1-(naphthalen-2-yl)ethanone (**3**) (94.4 mg, 0.554 mmol, 85%) as a colorless solid, the alcohol **4** (13.1 mg,

76.1 μmol, 12%) as a colorless solid, triphenylethoxysilane (**5 k**) (378 mg, 1.24 mmol, 95%) as colorless crystals, and triphenylsilanol (**6 k**; 7.9 mg, 2.9 μmol, 2%) as a colorless solid.

1-(Naphthalen-2-yl)ethanone (3): [CAS 93–08-3]: M.p. 54.1–55.7 °C; IR (ATR) $\nu =$ 3322, 3059, 2995, 1667, 1627, 1594, 1460, 1425, 1393, 1363, 1280, 1223, 1190, 1126, 1066, 1016, 960, 938, 900, 868, 832, 773, 753, 664, 651, 617 cm^{-1}; ^{1}H NMR (500 MHz, CDCl$_3$): $\delta =$ 2.74 (s, 3 H), 7.56 (ddd, $J =$ 8.5, 6.9, 1.6 Hz, 1 H), 7.61 (ddd, $J =$ 8.2, 6.9, 1.3 Hz, 1 H), 7.88 (d, $J =$ 7.3 Hz, 1 H), 7.90 (d, $J =$ 7.9 Hz, 1 H), 7.97 (d, $J =$ 8.2 Hz, 1 H), 8.04 (dd, $J =$ 8.5, 1.9 Hz, 1 H), 8.47 (s, 1 H); ^{13}C NMR and DEPT (126 MHz, CDCl$_3$): $\delta =$ 26.85 (CH$_3$), 124.04 (CH), 126.93 (CH), 127.93 (CH), 128.56 (CH), 128.62 (CH), 129.69 (CH), 130.35 (CH), 132.65 (C), 134.62 (C), 135.73 (C), 198.28 (C=O); MS (EI): m/z (%) = 170 (34, [M]$^+$), 156 (9), 155 (70), 128 (12), 127 (100), 126 (33), 115 (8), 101 (11), 87 (9), 77 (11), 75 (13), 74 (13), 63 (12); elemental analysis (%) calcd for C$_{12}$H$_{10}$O: C 84.68, H 5.92; found: C 84.93, H 6.15.

The spectroscopic data are in agreement with those reported in the literature.[12,14,44]

1-(Naphthalen-2-yl)ethanol (4): [CAS 7228–47-9]: M.p. 73.6–74.3 °C; IR (ATR) $\nu =$ 3300 (br), 3052, 3015, 2971, 2922, 2878, 1953, 1924, 1748, 1599, 1504, 1453, 1406, 1363, 1322, 1275, 1166, 1123, 1071, 1023, 950, 900, 861, 822, 772, 740, 703, 641, 619 cm^{-1}; ^{1}H NMR (500 MHz, CDCl$_3$): $\delta =$ 1.59 (d, $J =$ 6.3 Hz, 3 H), 1.92 (br s, 1 H), 5.08 (q, $J =$ 6.1 Hz, 1 H), 7.44–7.54 (m, 3 H), 7.80–7.87 (m, 4 H); ^{13}C NMR and DEPT (126 MHz, CDCl$_3$): $\delta =$ 25.29 (CH$_3$), 70.69 (CH), 123.94 (CH), 123.95 (CH), 125.94 (CH), 126.30 (CH), 127.81 (CH), 128.07 (CH), 128.47 (CH), 133.05 (C), 133.45 (C), 143.31 (C); MS (EI): m/z (%) = 172 (31, [M]$^+$), 157 (30), 130 (10), 129 (100), 128 (82), 127 (47), 126 (18), 115 (8), 102 (11), 77 (8), 75 (9), 74 (8), 63 (10), 43 (14); elemental analysis (%) calcd for C$_{12}$H$_{12}$O: C 83.69, H 7.02; found: C 83.84, H 7.11.

The spectroscopic data are in agreement with those reported in the literature.[12,14,45]

Triphenylethoxysilane (5 k): [CAS 1516–80-9]: M.p. 63.1–64.9 °C; IR (ATR) $\nu =$ 3131, 3050, 3008, 2968, 2922, 2899, 2874, 1960, 1898, 1825, 1775, 1725, 1617, 1590, 1567, 1473, 1457, 1427, 1389, 1336, 1306, 1272, 1158, 1115, 1075, 1027, 996, 946, 891, 856, 819, 767, 737, 709, 695 cm^{-1}; ^{1}H NMR (600 MHz, CDCl$_3$): $\delta =$ 1.26 (td, $J =$ 6.9, 0.8 Hz, 3 H), 3.89 (qd, $J =$ 7.0, 0.9 Hz, 2 H), 7.38–7.42 (m, 6 H), 7.42–7.47 (m, 3 H), 7.65 (dt, $J =$ 7.7, 1.1 Hz, 6 H); ^{13}C NMR and DEPT (151 MHz, CDCl$_3$): $\delta =$ 18.53 (CH$_3$), 59.89 (CH$_2$), 127.98 (6 CH), 130.10 (3 CH), 134.58 (3 CH), 135.52 (6 C); MS (EI): m/z (%) = 304 (34, [M]$^+$), 259 (23), 227 (98), 226 (77), 199, (48), 197 (23), 183 (100), 182 (25), 181 (54), 180 (16), 155 (13), 152 (16), 151 (10), 150 (55), 123 (19), 105 (28), 104 (13), 78 (12), 77 (34), 51 (13), 45 (10); MS (ESI, + 10 V): m/z 305.2 [M + H]$^+$; elemental analysis (%) calcd for C$_{20}$H$_{20}$OSi: C 78.90, H 6.62; found: C 79.21, H 6.45.

The spectroscopic data are in agreement with those reported in the literature.[46]

Triphenylsilanol (6 k): [CAS 791–31-1]: M.p. 154.5–156.6 °C; IR (ATR) $\nu =$ 3218 (br), 1962, 1884, 1821, 1772, 1660, 1613, 1589, 1567, 1472, 1457, 1426, 1332, 1304, 1263, 1187, 1116, 1069, 1026, 997, 850, 832, 737, 709, 694 cm^{-1}; ^{1}H NMR (600 MHz, CDCl$_3$): $\delta =$ 2.53 (br s, 1 H), 7.37–7.42 (m, 6 H), 7.43–7.47 (m, 3 H), 7.62–7.66 (m, 6 H); ^{13}C NMR and DEPT (151 MHz, CDCl$_3$): $\delta =$ 128.08 (6 CH), 130.28 (3 CH), 135.12 (6 CH), 135.25 (3 C); MS (EI): m/z (%) = 276 (48, [M]$^+$), 200 (19), 199 (100), 197 (16), 181 (12), 152 (11), 122 (15), 77 (22), 51 (13); elemental analysis (%) calcd for C$_{18}$H$_{16}$OSi: C 78.22, H 5.83; found: C 78.37, H 5.87.

The spectroscopic data are in agreement with those reported in the literature.[47]

Conflict of Interest

The authors declare no conflict of interests.

Keywords: iron · labeling studies · Mössbauer spectroscopy · oxidation · reaction mechanism

[1] a) T. Mukaiyama, T. Yamada, *Bull. Chem. Soc. Jpn.* **1995**, *68*, 17–35; b) C. Bolm, J. Legros, J. Le Paih, L. Zani, *Chem. Rev.* **2004**, *104*, 6217–6254; c) *Iron Catalysis in Organic Chemistry: Reactions and Applications* (Ed.: B. Plietker), Wiley-VCH, Weinheim, **2008**; d) *Catalysis without Precious Metals* (Ed.: R. M. Bullock), Wiley-VCH, Weinheim, **2010**; e) *Top. Organomet. Chem.* **2015**, *50*, 1–356 (Ed.: E. Bauer); f) I. Bauer, H.-J. Knölker, *Chem. Rev.* **2015**, *115*, 3170–3387; g) K. S. Egorova, V. P. Ananikov, *Angew. Chem. Int. Ed.* **2016**, *55*, 12150–12162; *Angew. Chem.* **2016**, *128*, 12334–12347; h) A. Fürstner, *ACS Cent. Sci.* **2016**, *2*, 778–789; i) E. B. Bauer, *Isr. J. Chem.* **2017**, *57*, 1131–1150; j) *Recent Advances in Iron Catalysis* (Ed.: H.-J. Knölker), MDPI, Basel, **2020**; k) S. Rana, J. P. Biswas, S. Paul, A. Paik, D. Maiti, *Chem. Soc. Rev.* **2021**, *50*, 243–472; l) T. Taniguchi, *Synlett* **2021**, *32*, 573–581.

[2] Selected examples: a) B. Gaspar, E. M. Carreira, *Angew. Chem. Int. Ed.* **2008**, *47*, 5758–5760; *Angew. Chem.* **2008**, *120*, 5842–5844; b) E. K. Leggans, T. J. Barker, K. K. Duncan, D. L. Boger, *Org. Lett.* **2012**, *14*, 1428–1431; c) S. W. M. Crossley, F. Barabé, R. A. Shenvi, *J. Am. Chem. Soc.* **2014**, *136*, 16788–16791; d) X. Ma, H. Dang, J. A. Rose, P. Rablen, S. B. Herzon, *J. Am. Chem. Soc.* **2016**, *139*, 5998–6007; e) J. C. Lo, D. Y. Kim, C.-M. Pan, J. T. Edwards, Y. Yabe, J. H. Gui, T. Qin, S. Gutiérrez, J. Giacoboni, M. W. Smith, P. L. Holland, P. S. Baran, *J. Am. Chem. Soc.* **2017**, *139*, 2484–2503; for reviews see:, f) M. D. Greenhalgh, A. S. Jones, S. P. Thomas, *ChemCatChem* **2015**, *7*, 190–222; g) S. W. M. Crossley, C. Obradors, R. M. Martinez, R. A. Shenvi, *Chem. Rev.* **2016**, *116*, 8912–9000.

[3] a) I. Tabushi, N. Koga, *J. Am. Chem. Soc.* **1979**, *101*, 6456–6458; b) M. Perrée-Fauvet, A. Gaudemer, *J. Chem. Soc. Chem. Commun.* **1981**, 874–875.

[4] Y.-I. Matsushita, T. Matsui, K. Sugamoto, *Chem. Lett.* **1992**, *21*, 1381–1384.

[5] T. Yamada, T. Mukaiyama, *Chem. Lett.* **1989**, *18*, 519–522.

[6] Y.-I. Matsushita, K. Sugamoto, T. Matsui, *Chem. Lett.* **1992**, *21*, 2165–2168.

[7] a) K. Kato, T. Mukaiyama, *Chem. Lett.* **1989**, *18*, 2233–2236; b) N. H. Taylor, E. J. Thomas, *Tetrahedron* **1999**, *55*, 8757–8768.

[8] a) N. Nagatomo, K. Koshimizu, K. Masuda, T. Tabuchi, D. Urabe, M. Inoue, *J. Am. Chem. Soc.* **2014**, *136*, 5916–5919; b) M. Nagatomo, K. Hagiwara, K. Masuda, M. Koshimizu, T. Kawamata, Y. Matsui, D. Urabe, M. Inoue, *Chem. Eur. J.* **2016**, *22*, 222–229.

[9] a) A. Zombeck, D. E. Hamilton, R. S. Drago, *J. Am. Chem. Soc.* **1982**, *104*, 6782–6784; b) T. Okamoto, S. Oka, *J. Org. Chem.* **1984**, *49*, 1589–1594; c) D. E. Hamilton, R. S. Drago, A. Zombeck, *J. Am. Chem. Soc.* **1987**, *109*, 374–379; d) T. Okamoto, Y. Sasaki, K. Sasaki, S. Oka, *Bull. Chem. Soc. Jpn.* **1987**, *60*, 4449–4450; e) M. Shimizu, H. Orita, T. Hayakawa, K. Takehira, *J. Mol. Catal.* **1989**, *53*, 165–172; f) T. Mukaiyama, S. Isayama, S. Inoki, K. Kato, T. Yamada, T. Takai, *Chem. Lett.* **1989**, *18*, 449–452; g) S. Inoki, K. Kato, T. Takai, S. Isayama, T. Yamada, T. Mukaiyama, *Chem. Lett.* **1989**, *18*, 515–518; h) S. Isayama, T. Mukaiyama, *Chem. Lett.* **1989**, *18*, 569–572; i) S. Isayama, T. Mukaiyama, *Chem. Lett.* **1989**, *18*, 1071–1074; j) H. Ogoshi, Y. Suzuki, Y. Kuroda, *Chem. Lett.* **1991**, *20*, 1547–1550; k) T. Tokuyasu, S. Kunikawa, K. J. McCullough, A. Masuyama, M. Nojima, *J. Org. Chem.* **2005**, *70*, 251–260.

[10] For a cobalt-catalyzed aldehyde-selective Wacker-type oxidation see: a) G. Zhang, X. Hu, C.-W. Chiang, H. Yi, P. Pei, A. K. Singh, A. Lei, *J. Am. Chem. Soc.* **2016**, *138*, 12037–12040; for iron-catalyzed aldehyde-selective Wacker-type oxidations, see: b) G.-Q. Chen, Z.-J. Xu, C.-Y. Zhou, C.-M. Che, *Chem. Commun.* **2011**, *47*, 10963–10965; c) A. D. Chowdhury, R. Ray, G. K. Lahiri, *Chem. Commun.* **2012**, *48*, 5497–5499; d) Y.-D. Du, C.-W. Tse, Z.-J. Xu, Y. Liu, C.-M. Che, *Chem. Commun.* **2014**, *50*, 12669–12672.

[11] B. Liu, F. Jin, T. Wang, X. Yuan, W. Han, *Angew. Chem. Int. Ed.* **2017**, *56*, 12712–12717; *Angew. Chem.* **2017**, *129*, 12886–12891.

[12] F. Puls, H.-J. Knölker, *Angew. Chem. Int. Ed.* **2018**, *57*, 1222–1226; *Angew. Chem.* **2018**, *130*, 1236–1240.

[13] J. G. Jones, M. V. Twigg, *Inorg. Chem.* **1969**, *8*, 2018–2019.

[14] F. Puls, P. Linke, O. Kataeva, H.-J. Knölker, *Angew. Chem. Int. Ed.* **2021**, *60*, 14083–14090; *Angew. Chem.* **2021**, *133*, 14202–14209.

[15] a) T. Mori, T. Santa, T. Higushi, T. Mashino, M. Hirobe, *Chem. Pharm. Bull.* **1993**, *41*, 292–295; b) C.-C. Guo, J.-X. Song, X.-B. Chen, G.-F. Jiang, *J. Mol. Catal. A* **2000**, *157*, 31–40; c) H. Ishikawa, D. A. Colby, S. Seto, P. Va, A. Tam, H. Kakei, T. J. Rayl, I. Hwang, D. L. Boger, *J. Am. Chem. Soc.* **2009**, *131*, 4904–4916; d) Poonam, P. Kumari, R. Nagpal, S. M. S. Chauhan, *New J. Chem.* **2011**, *35*, 2639–2646.

[16] a) R. F. Fritsche, G. Theumer, O. Kataeva, H.-J. Knölker, *Angew. Chem. Int. Ed.* **2017**, *56*, 549–553; *Angew. Chem.* **2017**, *129*, 564–568; b) C. Brütting, R. F. Fritsche, S. K. Kutz, C. Börger, A. W. Schmidt, O. Kataeva, H.-J. Knölker, *Chem. Eur. J.* **2018**, *24*, 458–470; c) A. Purtsas, O. Kataeva, H.-J. Knölker, *Chem. Eur. J.* **2020**, *26*, 2499–2508; d) A. Purtsas, S. Stipurin, O. Kataeva, H.-J. Knölker, *Molecules* **2020**, *25*, 1608; e) H.-J. Knölker, *Sitzungsberichte der Sächsischen Akademie der Wissenschaften zu Leipzig – Math.-naturwiss. Klasse*, Vol. 133, no. 4, S. Hirzel, Stuttgart/Leipzig, **2021**, pp. 1–30.

[17] a) C. Chatgilialoglu, D. Griller, M. Lesage, *J. Org. Chem.* **1988**, *53*, 3641–3642; b) C. Chatgilialoglu, C. Ferreri, Y. Landais, V. I. Timokhin, *Chem. Rev.* **2018**, *118*, 6516–6572.

[18] F. Puls, O. Kataeva, H.-J. Knölker, *Eur. J. Org. Chem.* **2018**, 4272–4276.

[19] a) D. Vonderschmitt, K. Bernauer, S. Fallab, *Helv. Chim. Acta* **1965**, *48*, 951–954; b) B. W. Dale, *Trans. Faraday Soc.* **1969**, *65*, 331; c) J. G. Jones, M. V. Twigg, *Inorg. Chem.* **1969**, *8*, 2120–2123; d) I. Collamati, *Inorg. Chim. Acta* **1979**, *35*, 303–304; e) C. Ercolani, F. Monacelli, G. Rossi, *Inorg. Chem.* **1979**, *18*, 712–716; f) C. Ercolani, G. Rossi, F. Monacelli, *Inorg. Chim. Acta Lett.* **1980**, *44*, L215–L216; g) D.-H. Chin, A. L. Balch, G. N. La Mar, *J. Am. Chem. Soc.* **1980**, *102*, 1446–1448; h) D.-H. Chin, G. N. La Mar, A. L. Balch, *J. Am. Chem. Soc.* **1980**, *102*, 4344–4350; i) D.-H. Chin, G. N. La Mar, A. L. Balch, *J. Am. Chem. Soc.* **1980**, *102*, 5945–5947; j) I. Collamati, *Inorg. Nucl. Chem. Lett.* **1981**, *17*, 69–73; k) A. B. P. Lever, S. Licoccia, B. S. Ramaswamy, *Inorg. Chim. Acta* **1982**, *64*, L87–L90; l) C. Ercolani, M. Gardini, F. Monacelli, G. Pennesi, G. Rossi, *Inorg. Chem.* **1983**, *22*, 2584–2589; m) A. L. Balch, Y.-W. Chan, R.-J. Cheng, G. N. La Mar, L. Latos-Grazynski, M. W. Renner, *J. Am. Chem. Soc.* **1984**, *106*, 7779–7785; n) C. Ercolani, M. Gardini, K. S. Murray, G. Pennesi, G. Rossi, *Inorg. Chem.* **1986**, *25*, 3972–3976; o) C. Ercolani, F. Monacelli, S. Dzugan, V. L. Goedken, G. Pennesi, G. Rossi, *J. Chem. Soc., Dalt. Trans.* **1991**, 1309–1315; p) R. Dieing, G. Schmid, E. Witke, C. Feucht, M. Dreßen, J. Pohmer, M. Hanack, *Chem. Ber.* **1995**, *128*, 589–598; q) J. Zhou, F. Wu, Z. Zhu, T. Xu, W. Lu, *Chem. Eng. J.* **2017**, *328*, 915–926; r) A. B. Sorokin, *Coord. Chem. Rev.* **2019**, *389*, 141–160.

[20] a) D. M. Kurtz Jr., *Chem. Rev.* **1990**, *90*, 585–606; b) L. Weber, G. Haufe, D. Rehorek, H. Hennig, *J. Chem. Soc. Chem. Commun.* **1991**, 502–503; c) L. Weber, M. Grosche, H. Hennig, G. Haufe, *J. Mol. Catal.* **1993**, *78*, L9–L13; d) M. J. Chen, D. E. Fremgen, J. W. Rathke, *J. Porphyrins Phthalocyanines* **1998**, *2*, 473–482; e) A. B. Sorokin, A. Tuel, *New J. Chem.* **1999**, *23*, 473–476; f) A. B. Sorokin, A. Tuel, *Catal. Today* **2000**, *57*, 45–59; g) C. Guo, Q. Peng, Q. Liu, G. Jiang, *J. Mol. Catal. A* **2003**, *192*, 295–302; h) C. Pérollier, C. Pergrale-Mejean, A. B. Sorokin, *New J. Chem.* **2005**, *29*, 1400–1403; i) E. V. Kudrik, P. Afansiev, D. Bouchu, J.-M. M. Millet, A. B. Sorokin, *J. Porphyrins Phthalocyanines* **2008**, *12*, 1078–1089; j) O. V. Zalomaeva, I. D. Ivanchikova, O. A. Kholdeeva, A. B. Sorokin, *New J. Chem.* **2009**, *33*, 1031–1037; k) H. M. Neu, M. S. Yusubov, V. V. Zhdankin, V. N. Nemykin, *Adv. Synth. Catal.* **2009**, *351*, 3168–3174; l) O. V. Zalomaeva, A. B. Sorokin, O. A. Kholdeeva, *Green Chem.* **2010**, *12*, 1076–1082; m) H. M. Neu, V. V. Zhdankin, V. N. Nemykin, *Tetrahedron Lett.* **2010**, *51*, 6545–6548; n) A. B. Sorokin, E. V. Kudrik, *Catal. Today* **2011**, *159*, 37–46; o) A. B. Sorokin, *Chem. Rev.* **2013**, *113*, 8152–8191; p) M. S. Yusubov, C. Celik, M. R. Geraskina, A. Yoshimura, V. V. Zhdankin, V. N. Nemykin, *Tetrahedron Lett.* **2014**, *55*, 5687–5690.

[21] a) K. J. Balkus Jr., A. G. Gabrielov, S. L. Bell, F. Bedioui, L. Roué, J. Devynck, *Inorg. Chem.* **1994**, *33*, 67–72; b) M.-S. Liao, T. Kar, S. M. Gorun, S. Scheiner, *Inorg. Chem.* **2004**, *43*, 7151–7161; c) M.-S. Liao, J. D. Watts,

Chemistry–A European Journal

Full Paper
doi.org/10.1002/chem.202102848

Chemistry Europe
European Chemical
Societies Publishing

M.-J. Huang, S. M. Gorun, T. Kar, S. Scheiner, *J. Chem. Theory Comput.* **2005**, *1*, 1201–1210.

[22] C. Colomban, E. V. Kudrik, D. V. Tyurin, F. Albrieux, S. E. Nefedov, P. Afanasiev, A. B. Sorokin, *Dalton Trans.* **2015**, *44*, 2240–2251.

[23] For Mössbauer spectroscopy of FePcF$_{16}$, see also: "Synthese und Charakterisierung ungewöhnlicher Phthalocyaninatometallkomplexe", U. Ziener, *Dissertation*, Eberhard-Karls-Universität Tübingen (Germany), **1995**.

[24] C. A. Melendres, *J. Phys. Chem.* **1980**, *84*, 1936–1939.

[25] a) R. Taube, H. Drevs, E. Fluck, P. Kuhn, K. F. Brauch, *Z. Anorg. Allg. Chem.* **1969**, *364*, 297–315; b) E. Fluck, R. Taube In *Developments in Applied Spectroscopy, Vol. 8* (Eds.: E. L. Grove), Springer, New York, **1970**, pp. 244–254; c) J. Blomquist, L. C. Moberg, L. Y. Johansson, R. Larsson, *J. Inorg. Nucl. Chem.* **1981**, *43*, 2287–2292.

[26] a) H. Volz, M. Hassler, H. Schäfer, *Z. Naturforsch.* **1986**, *41b*, 1265–1272; b) J. H. Zagal, *Coord. Chem. Rev.* **1992**, *119*, 89–136; c) M. H. Seo, D. Higgins, G. Jiang, S. M. Choi, B. Han, Z. Chen, *J. Mater. Chem. A* **2014**, *2*, 19707–19716; d) l. Gamba, Z. Codolà, J. Lloret-Fillol, M. Costas, *Coord. Chem. Rev.* **2017**, *334*, 2–24; e) X. Huang, J. T. Groves, *Chem. Rev.* **2018**, *118*, 2491–2553; f) Z. Chen, S. Jiang, G. Kang, D. Nguyen, G. C. Schatz, R. P. Van Duyne, *J. Am. Chem. Soc.* **2019**, *141*, 15684–15692.

[27] a) M. W. Peterson, D. S. Rivers, R. M. Richman, *J. Am. Chem. Soc.* **1985**, *107*, 2907–2915; b) F. Monacelli, *Inorg. Chim. Acta* **1997**, *254*, 285–290; c) I. A. Dereven'kov, S. S. Ivanova, E. V. Kudrik, S. V. Makarov, A. S. Makarova, P. A. Stuzhin, *J. Serb. Chem. Soc.* **2010**, *78*, 1513–1530.

[28] H.-J. Knölker, E. Baum, H. Goesmann, R. Klauss, *Angew. Chem. Int. Ed.* **1999**, *38*, 2064–2066; *Angew. Chem.* **1999**, *111*, 2196–2199.

[29] a) J. C. Lo, J. Gui, Y. Yabe, C.-M. Pan, P. S. Baran, *Nature* **2014**, *516*, 343–348; b) J. Gui, C.-M. Pan, Y. Jin, T. Quin, J. C. Lo, B. J. Lee, S. H. Spergel, M. E. Mertzman, W. J. Pitts, T. E. La Cruz, M. A. Schmidt, N. Darvatkar, S. R. Natarajan, P. S. Baran, *Science* **2015**, *348*, 886–891; c) P. Asgari, Y. Hua, A. Bokka, C. Thiamsiri, W. Prasitwatcharakorn, A. Karedath, X. Chen, S. Sardar, K. Yum, G. Leem, B. S. Pierce, K. Nam, J. Gao, J. Jeon, *Nat. Catal.* **2019**, *2*, 164–173.

[30] a) W. T. Grubb, *J. Am. Chem. Soc.* **1954**, *76*, 3408–3414; b) J. A. Cella, J. C. Carpenter, *J. Organomet. Chem.* **1994**, *480*, 23–26; c) M. C. Brochier Salon, P.-A. Bayle, M. Abdelmouleh, S. Boufi, M. N. Belgacem, *Colloids Surf. A: Physicochem. Eng. Aspects* **2008**, *312*, 83–91.

[31] a) M. Tilset, V. D. Parker, *J. Am. Chem. Soc.* **1989**, *111*, 6711–6717; b) R. Morris Bullock, E. G. Samsel, *J. Am. Chem. Soc.* **1990**, *112*, 6886–6898; c) D. C. Eisenberg, J. R. Norton, *Isr. J. Chem.* **1991**, *31*, 55–66; d) D. C. Eisenberg, C. J. C. Lawrie, A. E. Moody, J. R. Norton, *J. Am. Chem. Soc.* **1991**, *113*, 4888–4895; e) S. A. Green, S. W. M. Crossley, J. L. M. Matos, S. Vásquez-Céspedes, S. L. Shevick, R. A. Shenvi, *Acc. Chem. Res.* **2018**, *51*, 2628–2640; f) H. Jiang, W. Lai, H. Chen, *ACS Catal.* **2019**, *9*, 6080–6086; g) D. Kim, S. M. W. Rahaman, B. Q. Mercado, R. Poli, P. L. Holland, *J. Am. Chem. Soc.* **2019**, *141*, 7473–7485; h) S. L. Shevick, C. V. Wilson, S. Kotesova, D. Kim, P. L. Holland, R. A. Shenvi, *Chem. Sci.* **2020**, *11*, 12401–12422; i) S. Sarkar, K. P. S. Cheung, V. Gevorgyan, *Chem. Sci.* **2020**, *11*, 12974–12993; j) P. V. Kattamuri, J. G. West, *J. Am. Chem. Soc.* **2020**, *142*, 19316–19326; k) W. P. Thomas, S. V. Pronin, *Acc. Chem. Res.* **2021**, *54*, 1347–1359.

[32] a) M. Takeuchi, M. Kodera, K. Kano, Z. Yoshida, *J. Mol. Catal. A* **1996**, *113*, 51–57; b) T. Sugimori, S. I. Horike, S. Tsamura, M. Handa, K. Kasuga, *Inorg. Chim. Acta* **1998**, *283*, 275–278; c) for a review on radical addition reactions, see: R. W. Hoffmann, *Chem. Soc. Rev.* **2016**, *46*, 577–583.

[33] a) K. Kano, H. Takagi, M. Takeuchi, S. Hashimoto, Z.-I. Yoshida, *Chem. Lett.* **1991**, *3*, 519–522; b) J. Setsune, Y. Ishimaru, A. Sera, *Chem. Lett.* **1992**, *21*, 377–380; c) M. Takeuchi, H. Shimakoshi, K. Kano, *Organometallics* **1994**, *13*, 1208–1213; d) R. Poli, *C. R. Chim.* **2021**, *24*, 147–175.

[34] R. D. Arasasingham, A. L. Balch, C. R. Cornman, L. Latos-Grazynski, *J. Am. Chem. Soc.* **1989**, *111*, 4357–4363.

[35] S. Yokota, H. Fujii, *J. Am. Chem. Soc.* **2018**, *140*, 5127–5137.

[36] a) R. A. Baglia, J. P. T. Zaragoza, D. P. Goldberg, *Chem. Rev.* **2017**, *117*, 13320–13352; b) J. P. T. Zaragoza, T. H. Yosca, M. A. Siegler, P. Moënne-Loccoz, M. T. Green, D. P. Goldberg, *J. Am. Chem. Soc.* **2017**, *139*, 13640–13643; c) T. M. Pangia, C. G. Davies, J. R. Prendergast, J. B. Gordon, M. A. Siegler, G. N. L. Jameson, D. P. Goldberg, *J. Am. Chem. Soc.* **2018**, *140*, 4191–4194; d) V. Yadav, R. J. Rodriguez, M. A. Siegler, D. P. Goldberg, *J. Am. Chem. Soc.* **2020**, *142*, 7259–7264; for an example of an OH radical transfer by P-450, see: e) H. Kagawa, T. Takahashi, S. Ohta, Y. Harigaya, *Xenobiotica* **2004**, *34*, 797–810.

[37] M. Yoshida, M. Miura, M. Nojima, S. Kusabayashi, *J. Am. Chem. Soc.* **1983**, *105*, 6279–6285.

[38] G. A. Russell, *J. Am. Chem. Soc.* **1957**, *79*, 3871–3877.

[39] a) S. Campestrini, B. Meunier, *Inorg. Chem.* **1992**, *31*, 1999–2006; b) N. Safari, F. Bahadoran, *J. Mol. Catal. A* **2001**, *171*, 115–121; c) K. Schröder, K. Junge, B. Bitterlich, M. Beller, *Top. Organomet. Chem.* **2011**, *33*, 83–109; d) I. Y. Skobelev, E. V. Kudrik, O. V. Zalomaeva, F. Albrieux, P. Afansiev, O. A. Kholdeeva, A. B. Sorokin, *Chem. Commun.* **2013**, *49*, 5577–5579; for a review, see: e) K. A. Jørgensen, *Chem. Rev.* **1989**, *89*, 431–458.

[40] J. Meinwald, S. S. Labana, M. S. Chadha, *J. Am. Chem. Soc.* **1963**, *85*, 582–585.

[41] M. W. C. Robinson, A. M. Davies, R. Buckle, I. Mabbett, S. H. Taylor, A. E. Graham, *Org. Biomol. Chem.* **2009**, *7*, 2559–2564.

[42] G. R. Fulmer, A. J. M. Miller, N. H. Sherden, H. E. Gottlieb, A. Nudelman, B. M. Stoltz, J. E. Bercaw, K. I. Goldberg, *Organometallics* **2010**, *29*, 2176–2179.

[43] S. Kamusella, H.-H. Klauß, *Hyperfine Interact.* **2016**, *237*, 82.

[44] J. A. Marko, A. Durgham, S. L. Bretz, W. Liu, *Chem. Commun.* **2019**, *55*, 937–940.

[45] B. Ciszek, I. Fleischer, *Chem. Eur. J.* **2018**, *24*, 12259–12263.

[46] N. Luo, J. Ouyang, H. Wen, Y. Zhong, J. Liu, W. Tang, R. Luo, *Organometallics* **2020**, *39*, 165–171.

[47] K. Wang, J. Zhou, Y. Jiang, M. Zhang, C. Wang, D. Xue, W. Tang, H. Sun, J. Xiao, C. Li, *Angew. Chem. Int. Ed.* **2019**, *58*, 6380–6384; *Angew. Chem.* **2019**, *131*, 6446–6450.